

NASA TECHNICAL NOTE



NASA TN D-6047

2.1

LOAN COPY: RETURN
AFWL (WLOL)
KIRTLAND AFB, N

0132672



TECH LIBRARY KAFB, NM

NASA TN D-6047

EXPERIMENTAL INVESTIGATION OF
SINGLE PARTICLE BEHAVIOR IN
AN AXISYMMETRIC MAGNETIC FIELD

by Ronald J. Schertler

Lewis Research Center

Cleveland, Ohio 44135



0132672

1. Report No. NASA TN D-6047		2. Government Accession No.		3. Report No. 0132672	
4. Title and Subtitle EXPERIMENTAL INVESTIGATION OF SINGLE PARTICLE BEHAVIOR IN AN AXISYMMETRIC MAGNETIC FIELD				5. Report Date October 1970	
				6. Performing Organization Code	
7. Author(s) Ronald J. Schertler				8. Performing Organization Report No. E-5737	
				10. Work Unit No. 120-26	
9. Performing Organization Name and Address Lewis Research Center National Aeronautics and Space Administration Cleveland, Ohio 44135				11. Contract or Grant No.	
				13. Type of Report and Period Covered Technical Note	
12. Sponsoring Agency Name and Address National Aeronautics and Space Administration Washington, D.C. 20546				14. Sponsoring Agency Code	
				15. Supplementary Notes	
16. Abstract Nonrelativistic particle behavior for single interactions with an axisymmetric mirror magnetic field was experimentally investigated. Measurements were made to determine the fraction of an injected electron beam which was transmitted through the mirror region as a function of injection angle for a variety of operating conditions. Measurements were carried out for a range of the adiabatic parameter ϵ between 0.027 and 0.22. Over this range results showed that, within the experimental error of this investigation, particle behavior remained adiabatic.					
17. Key Words (Suggested by Author(s)) Adiabatic particle behavior; Nonadiabatic particle behavior; Single particle injection; Loss cone angle; Axisymmetric magnetic mirror; Electron injection			18. Distribution Statement Unclassified - unlimited		
19. Security Classif. (of this report) Unclassified	20. Security Classif. (of this page) Unclassified	21. No. of Pages 26	22. Price* \$3.00		

EXPERIMENTAL INVESTIGATION OF SINGLE PARTICLE BEHAVIOR IN AN AXISYMMETRIC MAGNETIC FIELD

by Ronald J. Schertler

Lewis Research Center

SUMMARY

Nonrelativistic particle behavior for single interactions with an axisymmetric mirror magnetic field was experimentally investigated. Measurements were made to determine the fraction of an injected electron beam which was transmitted through the mirror region as a function of injection angle for a variety of operating conditions. Measurements were carried out for a range of the adiabatic parameter ϵ between 0.027 and 0.22. Over this range results showed that, within the experimental error of this investigation, particle behavior remained adiabatic.

INTRODUCTION

The study of single, charged particle motion in static magnetic fields of mirror-type geometry can provide valuable information toward the understanding of the confinement of high temperature plasmas (refs. 1 to 6). Basic information of this type can also be applied in studies of the electric and magnetic properties of planetary radiation belts (ref. 7), and of the trapping of cosmic rays in interstellar magnetic fields (refs. 8 and 9).

This report describes an experimental investigation in which electrons in a relatively low strength axisymmetric magnetic field are used to simulate the behavior of high energy ions in high strength magnetic fields. Such information can be used, for example, to make an initial assessment of the trapping characteristics of high strength magnetic fields used to contain high temperature plasmas (ref. 4).

THEORY

Adiabatic Particle Behavior

The magnetic mirror principle is well-known. A charged particle gyrating along a magnetic field line in the direction of increasing field strength will experience a retarding force. If the velocity vector of the particle starts at a large enough angle with respect to the magnetic field line, the increasing magnetic field can act as a mirror and reflect the particle into a region of weaker field strength.

The equations of motion for a charged particle in a magnetic mirror field form a nonlinear set of coupled, second-order differential equations. Such equations do not have simple analytical solutions. From an examination of these equations, two constants of motion (the angular momentum and the total kinetic energy) can be found which provide general information about the particle motion. These constants do not, however, provide general criteria for determining the trapping characteristics of charged particles in a magnetic field.

Alfven (ref. 8) introduced an important simplification into the theory of charged particle motion in a nonuniform magnetic field. His simplification is referred to as First Order Orbit Theory. In the theory the concepts of guiding center motion and adiabatic invariants are used to predict particle motion in a steady or slowly varying magnetic field. The term adiabatic invariant refers to a quantity which remains essentially constant for slow changes in the magnetic field. A charged particle can have as many as three adiabatic invariants (ref. 2), depending on the shape and period of fluctuation of the magnetic field. The first of these invariants is the magnetic moment M_0 associated with the rotational component of the helical motion of the particle. The second invariant J_0 is associated with the longitudinal oscillation of the particle between the mirror points caused by the parallel gradient of the magnetic field. The third (or flux) invariant Φ_0 is associated with the azimuthal drift of the particle around the magnetic bottle as a consequence of the perpendicular gradient of the magnetic field. These three invariants are the lowest order terms of three asymptotic series of the form (ref. 2):

$$C_1 = M_0 + \epsilon M_1 + \epsilon^2 M_2 + \dots \quad (1)$$

$$C_2 = J_0 + \epsilon J_1 + \epsilon^2 J_2 + \dots \quad (2)$$

$$C_3 = \Phi_0 + \epsilon \Phi_1 + \epsilon^2 \Phi_2 + \dots \quad (3)$$

(All symbols are defined in the appendix.) The expansion parameter ϵ is referred to as the smallness or adiabatic parameter and the subscripted terms 1, 2, . . . , arise

from the series solution of the equations of motion. For steady-state, nonuniform magnetic fields, ϵ can be regarded as the ratio of the gyroradius r_g to the characteristic distance over which the magnetic field changes z_0 (ref. 2):

$$\epsilon = \frac{r_g}{z_0} = \frac{mv_{\perp}}{qB_{av}z_0} \quad (4)$$

where for simple magnetic mirror configurations, the distance over which the magnetic field changes can be represented by the axial distance z_0 between the minimum and maximum magnetic field strength locations. This axial distance is one-half the mirror coil separation distance. The average value of the magnetic field strength on axis may be written as

$$B_{av} = \frac{1}{2} (B_{max} + B_{min}) \quad (5)$$

Actually these three asymptote series (eqs. (1) to (3)) are the invariants of the particle motion. However, because the higher order terms in these series have been derived only for a few special cases, the series cannot generally be used to predict the conditions for adiabatic motion. Consequently, the magnitude of ϵ is generally used as a guide to predict the conditions of particle confinement. If ϵ is much smaller than unity ($\epsilon \ll 1$), only the zero-order terms of the series are significant and particle containment is associated, for example, with the constancy of M_0 .

By equating the total energy of the particle at the midplane with that of the particle at the mirror reflection position, and by using the fact that the magnetic moment M_0 is a constant, a loss cone can be defined as described in the following paragraphs.

Figure 1 depicts the loss cone in a simple magnetic mirror configuration for a par-

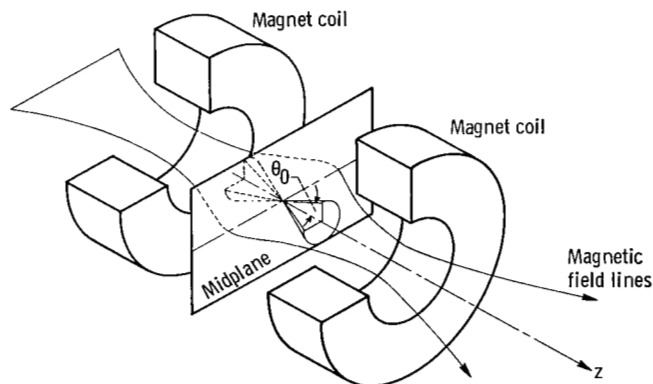


Figure 1 - Schematic of loss cone for point located at midplane and on axis of an axisymmetric mirror field.

ticle on axis at the midplane. If the particle velocity vector is oriented outside this cone, the motion of the particle is such that it will be reflected before it reaches the maximum value of the magnetic field B_{\max} .

Conversely, the particle will escape from the system if its velocity vector lies inside the loss cone. The half-angle of the loss cone, as shown in figure 1, is given by

$$\theta_0 = \sin^{-1}(R_m)^{1/2} \quad (6a)$$

where the mirror ratio is $R_m = B_{\min}/B_{\max}$. The magnetic field strength at the position of the particle is B_{\min} . The magnetic field B_{\max} is located on axis in the plane of the coil.

In general, the loss cone half-angle is a function of particle position and can be expressed as

$$\theta_0 = \sin^{-1}\left(\frac{B_0}{B_{\max}}\right)_{R,z}^{1/2} \quad (6b)$$

where R and z are the radial and axial positions of the particle, respectively; and the magnetic field at the position of the particle is B_0 .

The loss cone half-angle θ_0 can also be displayed in velocity space in the manner shown in figure 2. In this representation the loss cone half-angle is

$$\theta_0 = \tan^{-1}\left(\frac{v_{\perp}}{v_{\parallel}}\right)_0 \quad (6c)$$

where $(v_{\perp})_0$ and $(v_{\parallel})_0$ are the velocity components perpendicular and parallel to the magnetic field lines, respectively. Because the magnetic field strength changes as a function of position, the loss cone increases as the particle moves away from the midplane. In the plane where $B_0 = B_{\max}$, the loss cone fills all velocity space and θ_0 is equal to 90° . From these equations it can be seen that the particle confinement depends only on the ratios of particle velocity (or energy) components and on the magnetic field strengths.

Nonadiabatic Particle Behavior

If the particle motion is adiabatic (i. e., $\epsilon \ll 1$), the particle may be trapped for many reflections. As ϵ increases, the particle motion can no longer be adequately described by First Order Orbit Theory and the motion is called nonadiabatic. As illus-

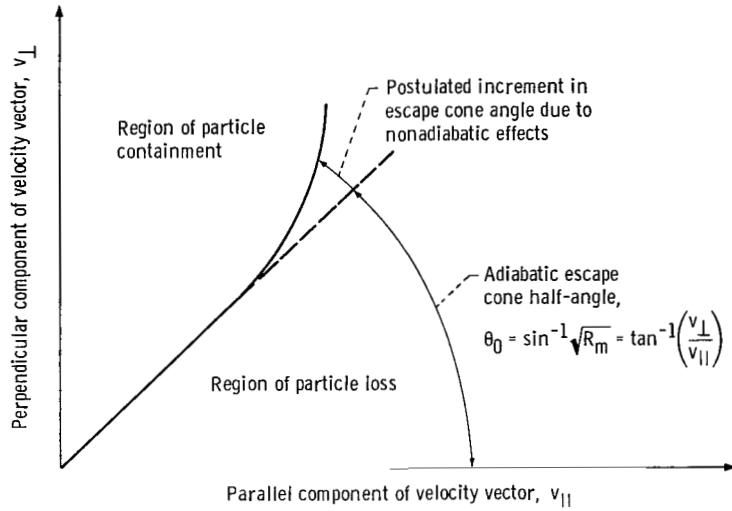


Figure 2. - Schematic diagram in velocity space of region of experimental investigation for any constant average magnetic field strength and magnet coil separation.

trated in figure 2, the loss cone associated with nonadiabatic particle motion may be greater than that predicted by adiabatic theory (ref. 10). Previous investigations have examined various aspects of adiabatic and nonadiabatic particle behavior in a magnetic mirror configuration (refs. 10 to 18). Most of these experiments have been concerned with the prolonged confinement of particles (i. e., multiple reflections). Any reduction in confinement time as the magnetic field strength was reduced was usually attributed to nonadiabatic particle behavior.

For multiple particle reflection ($\sim 10^9$), Gibson, Jordan, and Lauer (ref. 12) found a critical value of ϵ exists ($\epsilon = 0.06$) above which adiabatic theory is no longer valid and the particle motion becomes nonadiabatic. In a numerical study of the cumulative effects of particle reflection in a mirror system (ref. 10), it was found that nonadiabatic behavior can lead to particle loss after only a few reflections from the mirror regions.

Roth (ref. 13) has analytically and experimentally examined the behavior of non-relativistic charged particles which interact only once with a magnetic mirror region. Based on his investigation, enhanced particle loss attributed to nonadiabatic behavior was found to occur according to the following relation:

$$R_m \leq [2.87 \epsilon \exp(-0.0075 a)]^{0.388} \exp(-0.167a) \quad (7)$$

where a is a nondimensional radius, $\pi R/z_0$. For given values of R_m , R , and z_0 , a critical value of ϵ can be obtained. The particle behavior is predicted to be nonadiabatic for values of ϵ greater than the critical value. Figure 3 shows the critical value

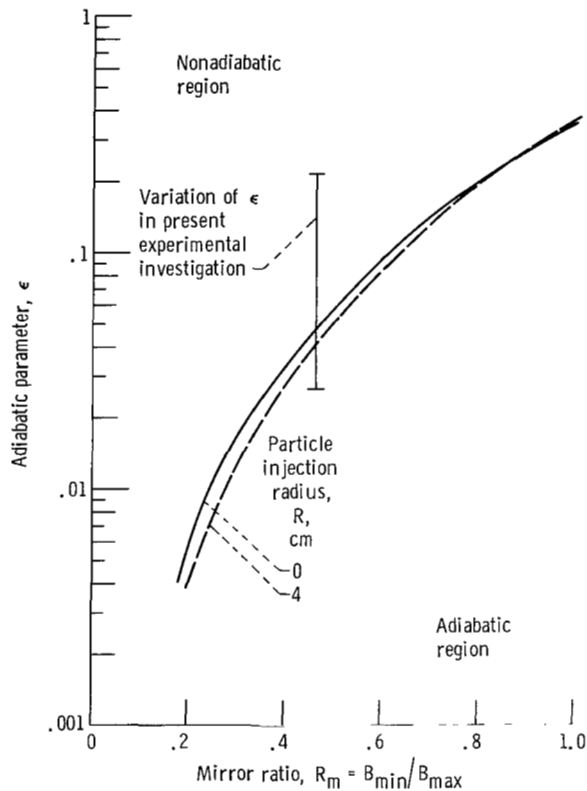


Figure 3. - Critical value of adiabatic parameter ϵ as function of mirror ratio (as calculated from ref. 13) Axial distance between regions of maximum and minimum axial magnetic field strength, 23 centimeters.

of ϵ from equation (7) as a function of mirror ratio for two different radial positions of the present experiment. Also shown on the figure is the range of ϵ that was investigated in the present experiment for a mirror ratio of 0.465. According to figure 3, for the conditions of the experiment a high degree of trapping should be expected for $\epsilon = 0.02$, and less trapping should occur for $\epsilon = 0.2$.

An alternative way of presenting the effect of particle velocity and average magnetic field strength on ϵ is shown in figure 4. This figure shows three curves corresponding to three beam accelerating voltages (particle velocities) used in this experiment. In calculating ϵ from equation (4), the velocity perpendicular to the magnetic field lines was assumed to be equal to the total velocity of the electron beam. Using the total velocity in the calculation of ϵ allows the results of the present experiment to be compared with the results of other experiments where only the total particle velocity is known. This results in a slightly larger value of ϵ than given by equation (4) for electrons injected near the loss cone angle at the midplane.

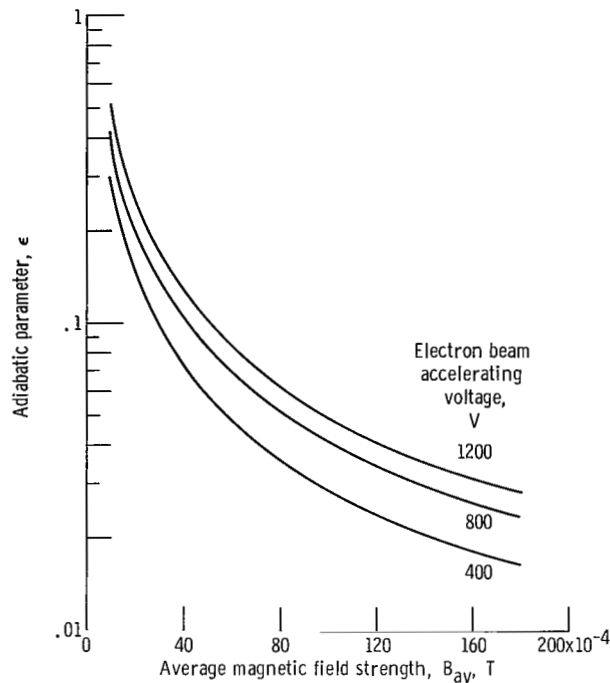


Figure 4. - Adiabatic parameter as function of average field strength for a range of beam accelerating voltages.

In summary then, although previous experiments have examined various aspects of single particle behavior, the experiments have not been of sufficient detail to establish the shape of the loss cone as a function of injection angle for nonadiabatic particle behavior. In this report the transmission characteristics of an electron beam were used to investigate this phenomenon.

APPARATUS

Vacuum Facility

The experimental apparatus was mounted from the end cap of a vacuum facility 3 meters in diameter and 5.8 meters long (ref. 19). Figure 5 is a cutaway view of the vacuum pumping system and experiment. The facility was evacuated by six 50-cubic-meter-per-second oil diffusion pumps. The diffusion pumps were backed by a 142-cubic-meter-per-minute lobe-type blower. The blower, in turn, was backed by a pair of 17-cubic-meter-per-minute mechanical pumps. Liquid nitrogen cooled, chevron-type traps were located between the diffusion pumps and the main vacuum chamber to prevent pump oil backstreaming. Pressure measurements were made on the axis and at various loca-

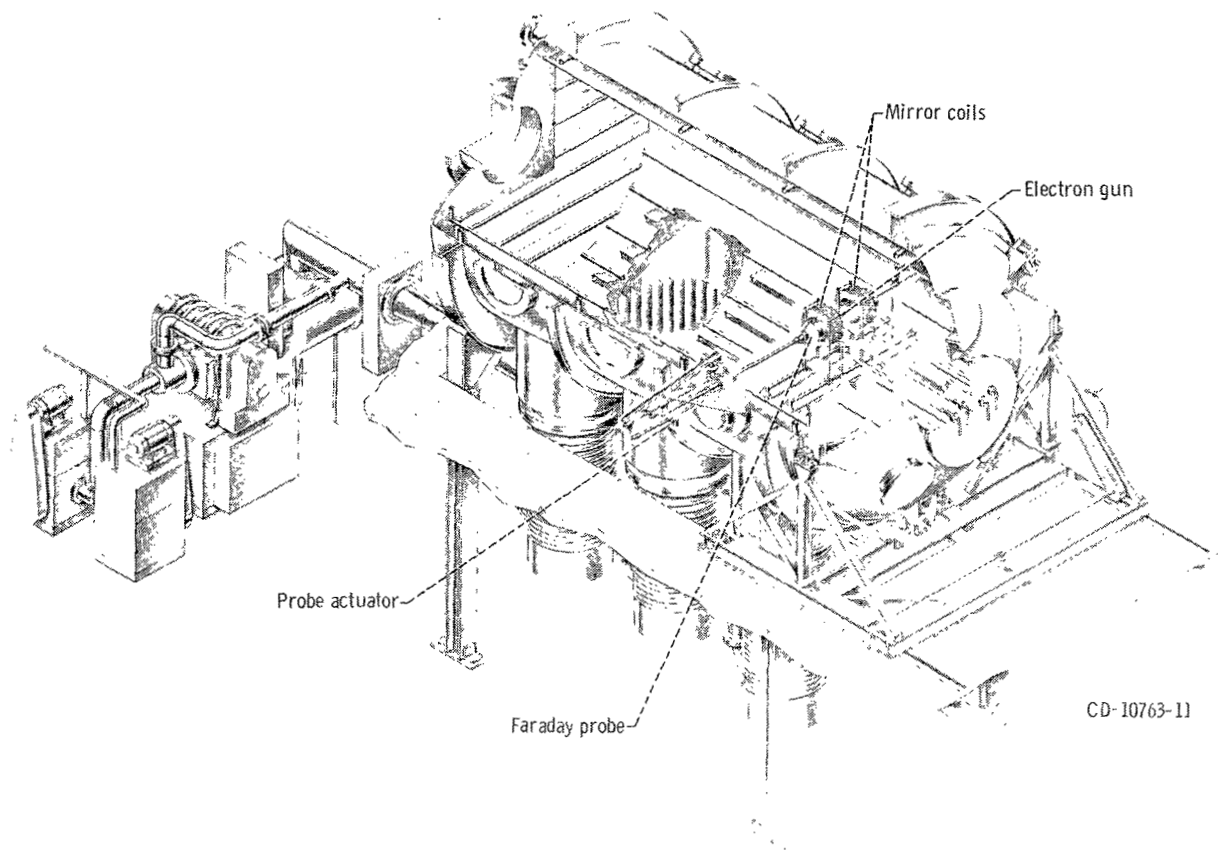


Figure 5. - Cutaway view of 3-meter-diameter, 5.8-meter-long vacuum tank, showing experiment location.

tions along the walls of the vacuum chamber. With cryogenic pumping used in conjunction with the other pumps, pressures of approximately 3.0×10^{-8} torr were maintained during the experimental runs.

Experimental Apparatus

The experimental apparatus as mounted in the vacuum facility is shown in figure 6. The screening used to maintain all surfaces at a constant electrical potential has been removed. The two magnet coils generate an axisymmetric double-mirror magnetic field. Typically, for a mirror ratio of 0.465 and a current of 500 amperes in each coil, the maximum magnetic field strength on axis was approximately 0.2 tesla. The electron gun is shown mounted on the axis of the coils at the midplane of the magnetic bottle. One of the Faraday cups used for particle diagnostics can be seen at the left.

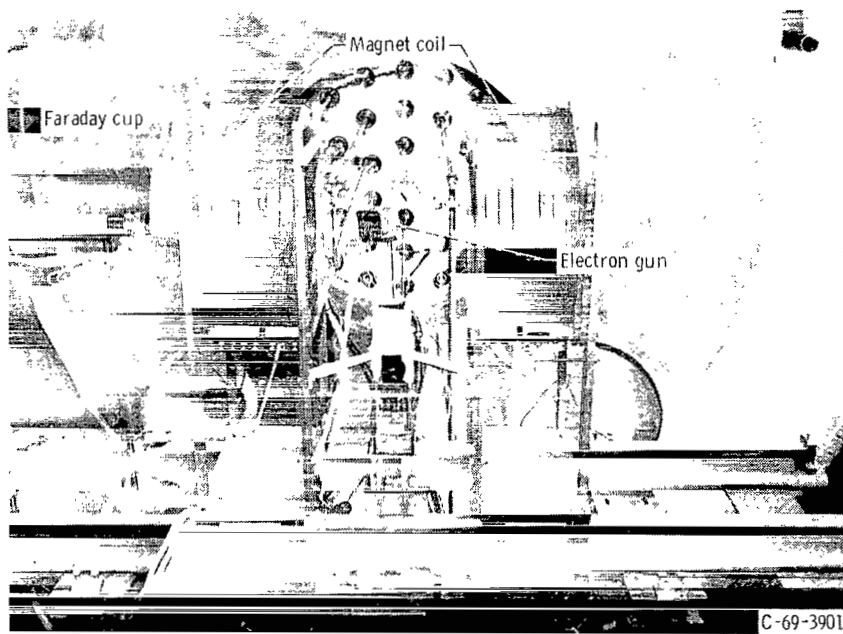


Figure 6. - Experiment mounted in vacuum facility.

Magnet Coils

Each magnet coil consists of 98 turns of copper tubing in a pancake arrangement. Each coil has an internal diameter of 26.6 centimeters, an outer diameter of 42.7 centimeters, and a width of 15.0 centimeters. The conductor used was 0.87 by 0.91 centimeter rectangular, oxygen-free-copper tubing with an internal water cooling channel 0.51 centimeter in diameter. Glass tape impregnated with epoxy resin provides the electrical insulation between the conductors.

One of the requirements for proper operation of this experiment was to maintain the background pressure less than 1.0×10^{-7} torr in order to minimize electron scattering effects caused by residual gases. The thermal outgassing rate of the glass-tape - epoxy insulation had been measured previously (ref. 20) to determine the maximum outgassing load produced by the coils under various operating conditions. For coil insulation temperatures less than 40° C, the outgassing rate was sufficiently low (less than 10^{-4} torr-cm³/cm²/sec), that the pumping system could maintain the chamber pressure below 10^{-7} torr. Water flowing through the internal channel of the conductor was used to maintain the coil temperatures below 40° C.

Figure 7 is an iron filing map of a cross section of an axisymmetric mirror field with $R_m = 0.465$. A mirror region is formed in the center of each coil as shown by the convergence of the flux lines. The magnetic field strength of this type of open-ended

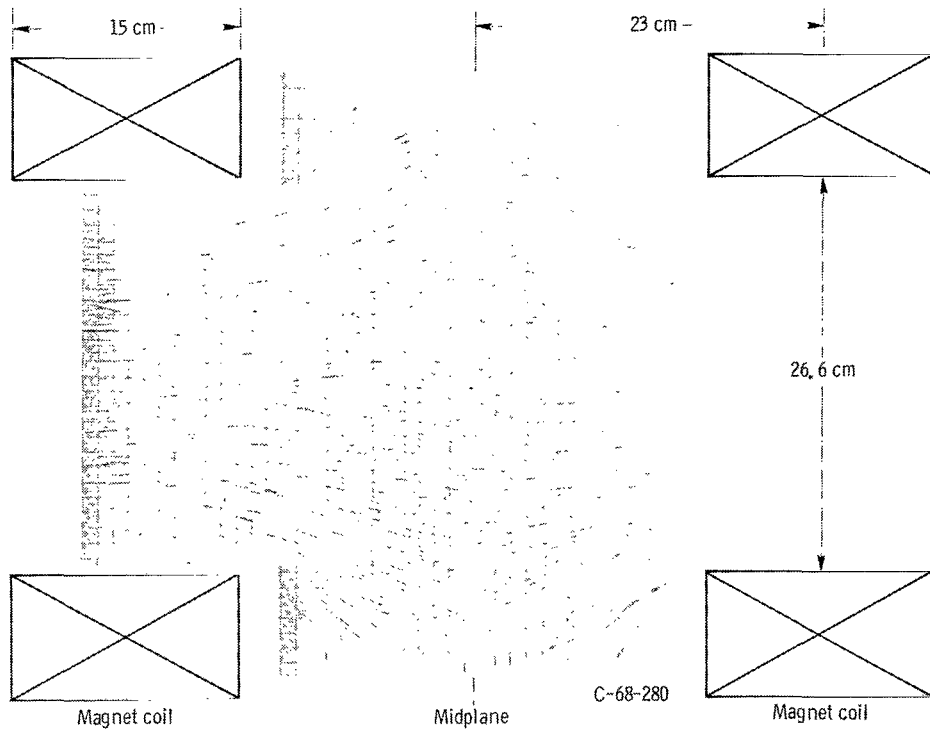


Figure 7. - Iron filing map of axisymmetric mirror magnetic field.

system increases both with axial distance from the midplane and with radial distance from the axis. A normalized plot of the magnetic field strength as a function of axial distance, for various radial positions, is shown in figure 8. Calculated and experimental values are compared for $R = 0$. The calculated values were obtained by the use of a computer program (ref. 21) which treats a magnet coil as a superposition of the fields of four appropriately placed, semi-infinite solenoids with zero inner radius. The experimental values were obtained with a Hall probe. Overall accuracy was ± 2 percent. Experimental values agree closely with calculated values.

The radial and axial magnetic field profile measurements, along with iron filing maps, were used to locate accurately both the midplane and the magnetic axis of the mirror configuration. In addition, these magnetic field measurements provided experimental values for the parameters z_0 , B_0 , and R_m .

Electron gun. - The electron gun used in this investigation was assembled from a commercially available kit (ref. 22). A cutaway view of the electron gun is shown in figure 9. Hole locations in the nonmagnetic plates were accurate to within ± 0.0025 centimeter. Ceramic rings were used to maintain precise interelectrode spacings. The final electron gun assembly was held together by alumina rods inserted through mounting holes in the electrodes and secured by slip-on wire retainers. The complete structure had a

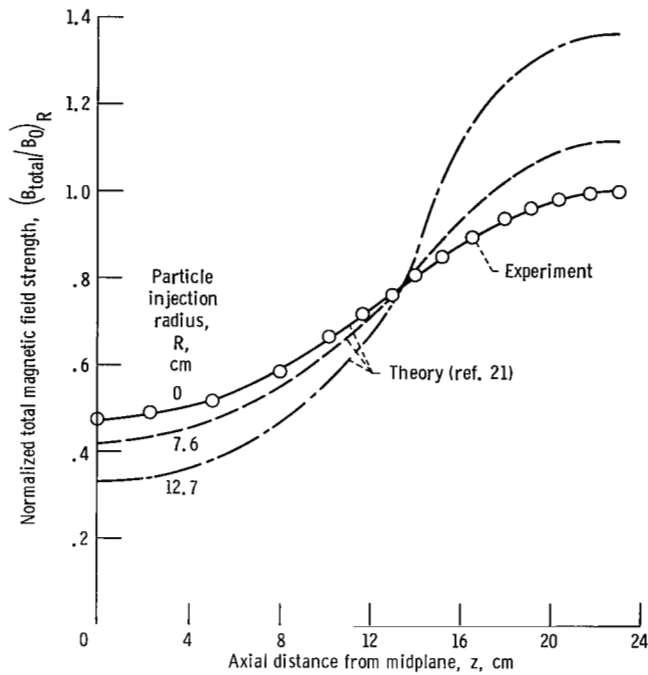


Figure 8. - Comparison of theoretical and experimental values of normalized magnetic field profiles. Axial distance between maximum and minimum axial magnetic field strength locations, 23 centimeters; mirror ratio on magnet axis, 0.465.

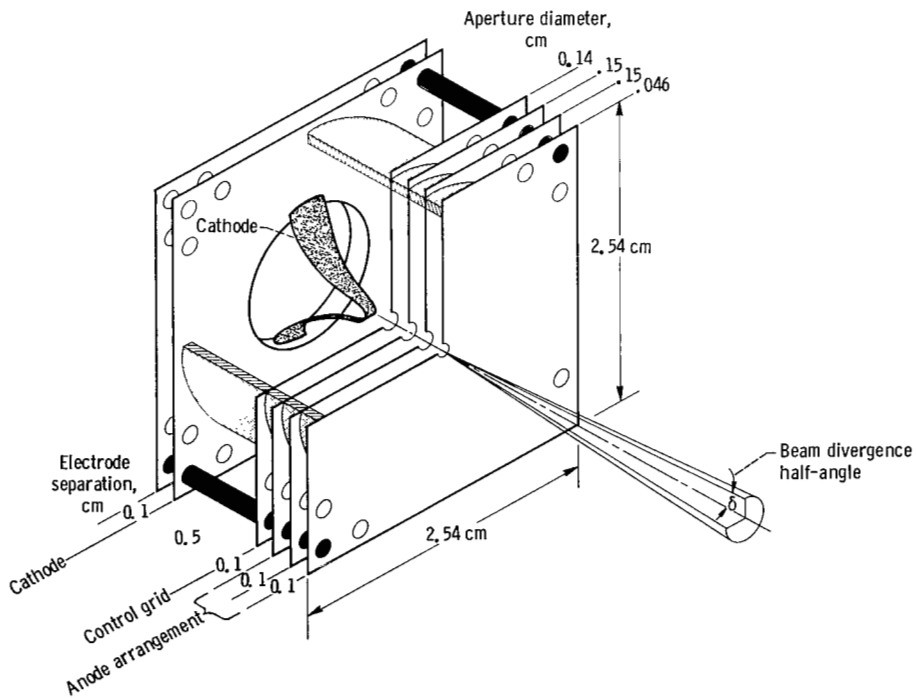


Figure 9. - Cutaway view of electron gun.

low thermal mass and could operate at high temperature while maintaining component alinement. The use of this gun allowed different electrode configurations to be assembled and tested while maintaining alinement and reassembly accuracy.

The cathode was fabricated from a 0.0025-centimeter-thick tantalum ribbon. The cathode was tapered in the center to a width of approximately 0.1 centimeter to provide a small emission region. During operation the cathode was resistively heated to approximately 2000 K by a current of a few amperes. The cathode was biased negatively with respect to ground at three operating voltages, -370, -770, and -1170 volts.

The emission current was controlled by biasing the control grid negative with respect to the cathode. The anode consisted of three electrodes in an Einzel lens arrangement. The first and third electrodes were maintained at +30 volts. The middle electrode was biased to near cathode potential. This type of anode arrangement resulted from extensive bell-jar testing. A narrow angle electron beam could be maintained over a wide range of beam accelerating voltage. The effect on the experimental results of the small beam divergence half-angle δ is discussed in a later section.

Electron gun alinement. - The electron gun was mounted and alined so that it could be rotated about a vertical axis passing through the final gun electrode, resulting in the beam directions defined by the angles $\pm\alpha$ shown in figure 10. The gun could be positioned at any desired injection radius R at the midplane. The injection angle α is references to the local direction of the magnetic field lines. (At the midplane, the local direction of the field lines is parallel to the magnetic axis of the mirror field.)

The gun was alined with respect to the magnet axis to within an accuracy of $\pm 1/2^\circ$. This alinement was accomplished by using a mirror, located parallel to the final anode of the gun, to superimpose the reflection of a cathetometer eyepiece onto the eyepiece itself. The cathetometer was previously alined with respect to the magnet axis. The

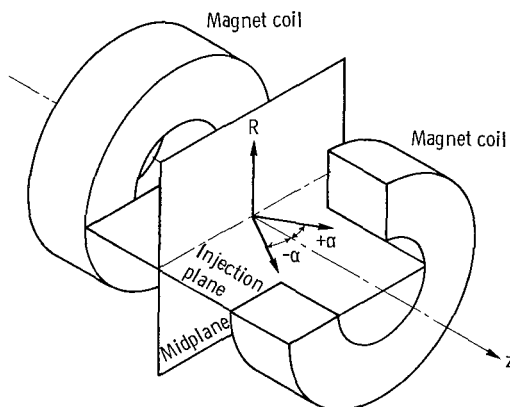


Figure 10. - Schematic of injection geometry.

electron gun was positioned at various injection angles by using a special drive motor. The overall accuracy and repeatability of this angular positioning system was within $\pm 1^\circ$.

Instrumentation

Figure 11 is a schematic diagram of the principal experimental equipment. Current measurements were made with a 24-centimeter-diameter Faraday cup collector mounted on a movable mount. To ensure that the electrons did not undergo multiple reflections, a second Faraday cup, 24 centimeters in diameter, was positioned directly behind the electron gun. The screen shown in figure 11 was used to provide a constant potential

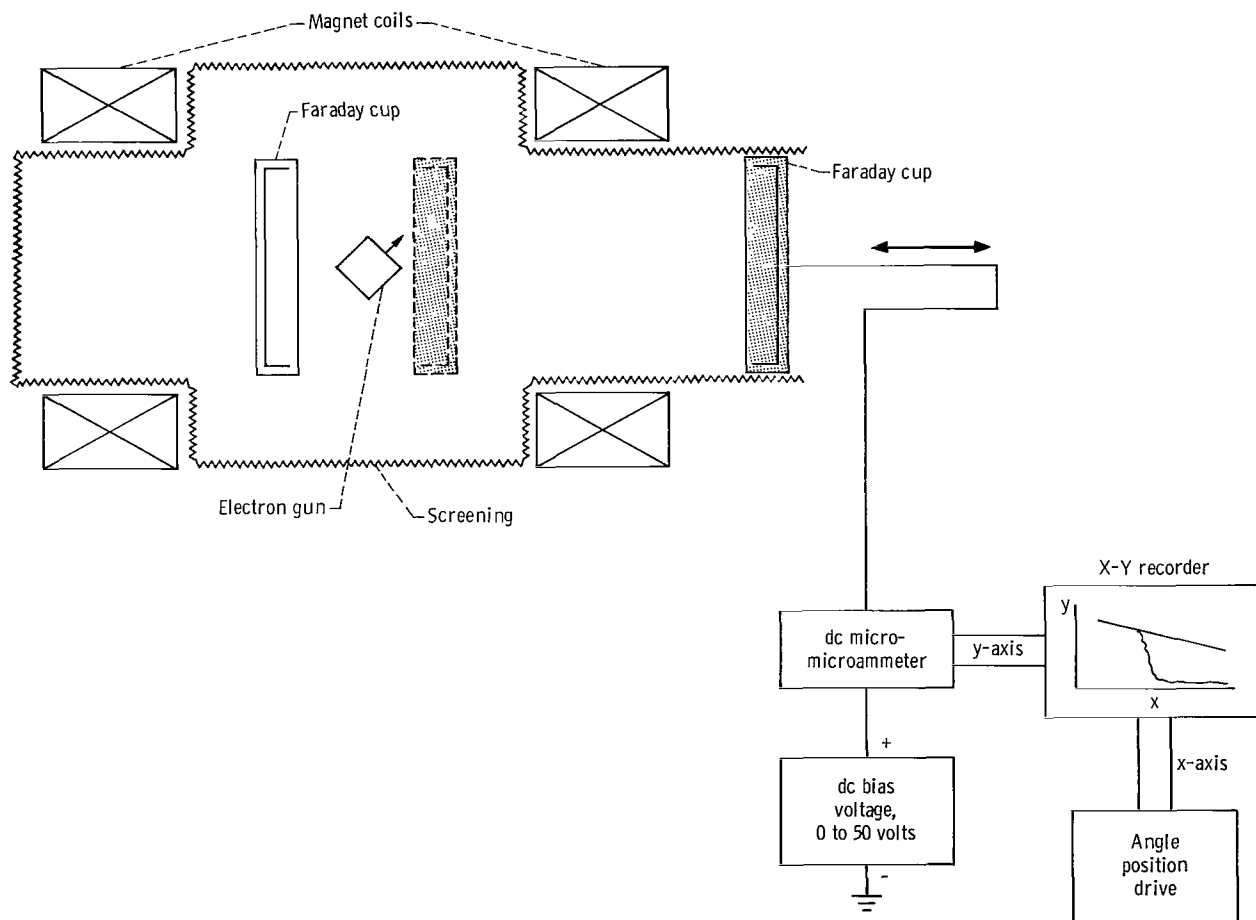


Figure 11. - Schematic diagram of principal experiment equipment.

surface (+30 V bias) and to shield the electron beam from any possible extraneous electric fields.

Several techniques were used to ensure low secondary emission from the collector surfaces. The Faraday cup was lined with aluminum honeycomb which had an average length-to-diameter ratio of 4. Next, fine tungsten fibers were placed inside the honeycomb structure. Finally, the whole structure was coated with a colloidal suspension of carbon powder which provided a surface with a low electron backscattering coefficient. The Faraday cup was then positively biased to approximately 30 volts with respect to ground.

The electron gun was mounted inside a metal housing which intercepted part of the electron beam reflected from the mirror region. The electron gun emission current was 1.0 microampere or less to ensure that the effects of space charge within the beam could be neglected. The metal housing was also coated with colloidal carbon and positively biased to 30 volts to minimize secondary electron emission. Several magnetic shielding configurations were tried for the electron gun housing but none were used. All of them significantly distorted the magnetic field in front of the gun. This distortion prevented an accurate measurement of the injection angle between the electron beam velocity vector and the magnetic field lines.

PROCEDURE

The fraction of the total electron beam transmitted through the ends of the magnetic mirror was used to provide information about the loss cone angle. Transmission measurements were recorded as a function of beam radial position and α over a range of the adiabatic parameter ϵ . The fraction of the current transmitted through the mirrors can be expressed as

$$T(\alpha, R, R_m, \epsilon) = \frac{I_O}{I_I} \quad (8)$$

The current I_O was measured at a position 3 centimeters outside the magnetic mirror region. The axial position of the Faraday cup outside the mirror region was not critical as long as the gyrations of the electron did not carry it beyond the edge of the Faraday cup. For example, under some circumstances the electrons miss the cup because the magnetic field decreases rapidly from the mirror region, resulting in an increase in the electron gyroradius. This situation was carefully avoided.

The current I_I was measured approximately 1 centimeter in front of the electron gun. This location ensured that the total beam current was measured and that no elec-

trons would be reflected before reaching the Faraday cup. Because I_I is not constant but decreases with increasing injection angle α , due to the influence of the magnetic field in the gun itself, the transmission fraction (eq. (8)) was always compared at the same injection angle.

Current measurements were recorded by a dc micro-microammeter and displayed as a function of injection angle α on the X-Y recorder shown schematically in figure 11. Figure 12 shows two sample curves of collector current as a function of injection angle.

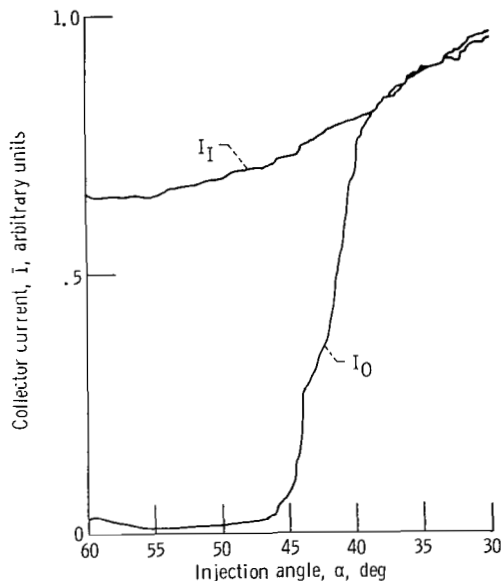


Figure 12. - Sample data from X-Y recorder.

The upper curve is a measure of the relative emission current taken directly in front of the electron gun inside the mirror field. The lower curve was recorded at a Faraday cup position outside the mirror region and is the current transmitted through the mirror. With a fixed magnetic field configuration (R_m and z_0 constant), the transmission characteristic as a function of injection angle was investigated for a range of ϵ by varying either the electron beam accelerating voltage V_A or the magnetic field strength B .

RESULTS AND DISCUSSION

Effect of Electron Gun Beam Divergence

It was found that the electron beam divergence had an effect on the experimental data. For clarity this effect will be discussed before examining the transmission data.

With no angular beam distribution, transmission through the bottle would abruptly fall to zero at an injection angle equal to the loss core angle. The occurrence of beam divergence, however, results in a less abrupt change in transmission characteristics. An analysis of this effect for a range of electron gun voltages and currents is necessary to be able to interpret the data.

In a separate calibration experiment, the beam divergence half-angle δ was measured in a bell-jar vacuum facility using the electron gun shown in figure 9 and a scanning Faraday cup with a slit aperture as described by Harker (ref. 23). Moss (ref. 24) points out that in narrow angle electron guns, the current distribution is very closely Gaussian in shape. In addition, if the slit width is small compared with the beam size, the shape of the current distribution obtained from a scanning slit is exactly equal to the angular distribution resulting from scanning the beam with an infinitesimal pinhole aperture.

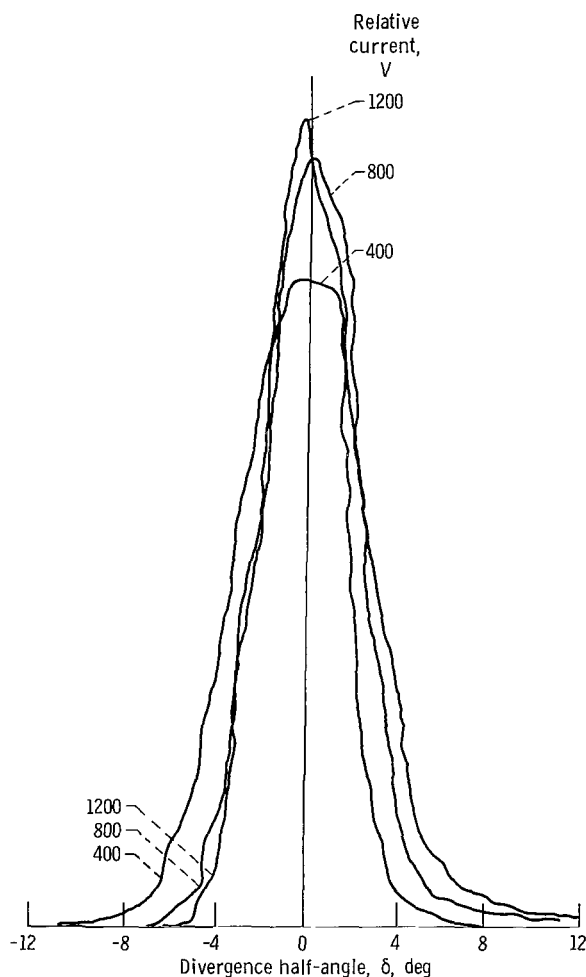


Figure 13. - Electron beam angular divergence.

Beam divergence results from the calibration experiment for beam accelerating voltages of 400, 800, and 1200 volts are presented in figure 13. A scanning slit width of 0.025 centimeter and a slit length of approximately 13 centimeters were utilized. The slit was positioned 11.5 centimeters from the anode of the electron gun. The electron beam current was approximately 1.0 microampere. The current was plotted on an X-Y recorder as a function of lateral slit position. The slit width was sufficiently small so that these measurements reflect the true Gaussian shape of the beam. The effect of beam divergence on the measurement of particle behavior in the magnetic mirror can be determined from these electron beam current profiles. The beam angular distribution must be related to the local direction of the magnetic field lines in order to determine the fraction of the total beam current which lies inside the adiabatic loss cone. To analyze the effect, the beam current distribution curve was approximated by a superposition of rectangular distributions, as shown in figure 14. These distributions were symmetric about the beam axis. At a given injection angle in the main experiment, the fraction of current which fell within the adiabatic loss cone angle was easily found by geometric

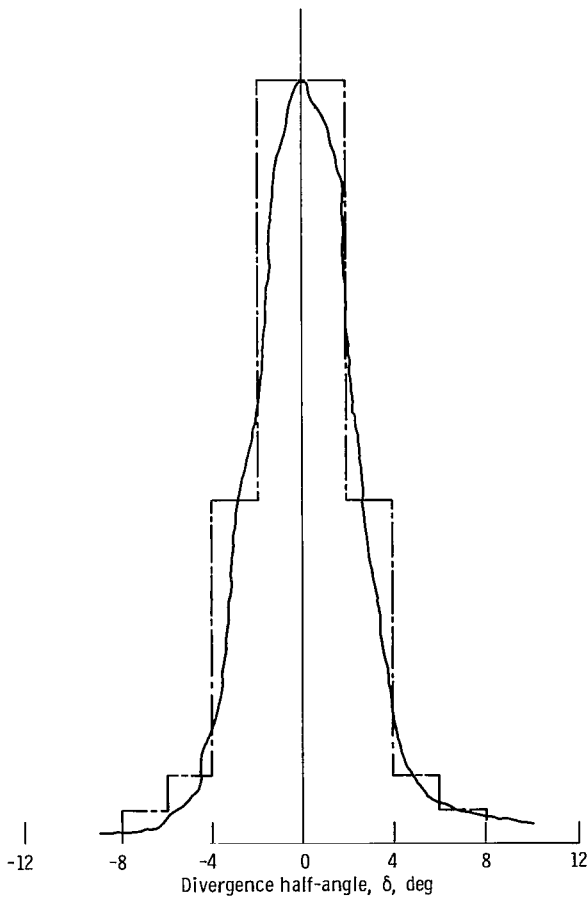


Figure 14. - Rectangular approximation of 800-volt distribution.

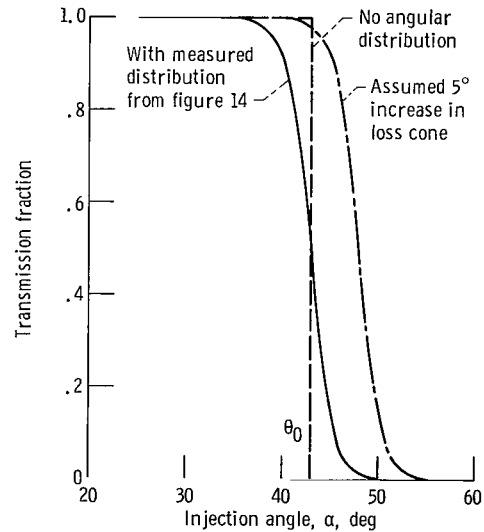


Figure 15. - Effect of beam distribution on fraction of beam transmitted through the mirror region as function of beam injection angle for 800-volt accelerating voltage and mirror ratio on magnet axis of 0.465.

projection. A typical result of this calculation is shown and compared in figure 15 with two other cases. For an electron beam with no angular distribution, the transmission falls to zero at an injection angle equal to the loss cone angle (dashed line). The loss cone angle was calculated in this case from equation (6a) for a mirror ratio of 0.465. Zero transmission indicates total particle reflection. For the beam angular distribution approximation of figure 14, the transmission decreases less abruptly (solid curve). Also shown for comparison is the effect on transmission of a possible 5° increase in the loss cone angle (broken line). Such an increase could result if the particle motion in the magnetic bottle became nonadiabatic. This curve shows that the shape of the transmission curve remains the same as that for the adiabatic case but is displaced toward increased injection angles.

Transmission Measurements

Transmission measurement results for electrons which interact only once with the magnetic mirror are shown in figures 16(a) to (c).

In figure 16(a), transmission results are presented for electrons injected on axis ($R = 0$) at the midplane. These results are presented for three different beam accelerating voltages and for the corresponding range of magnetic field strengths. Figures 16(a-1), (a-2), and (a-4) show the results for positive injection angles, while figure 16(a-3) is for negative angles. For electrons injected on the axis with positive injection angles, the helix formed by the gyrating electron motion remained above the magnet axis; while for negative angles, the electrons remained below the magnetic axis. The theoretical curve obtained from considering the beam divergence and a loss cone angle equal to 43° ($R_m = 0.465$) is also plotted on each figure. The experimental data show a spread of approximately 2° but correspond closely with the transmission fraction predicted theoretically from beam divergence measurements. The results for negative injection orientations (fig. 16(a-3)) also agree closely with the predicted transmission fraction and verify that symmetry was obtained. The range of ϵ for these results extended from approximately 0.027 to 0.22. For this range of ϵ , contrary to what was expected, the loss cone did not increase with ϵ , at least within the 2° spread of the data; that is, nonadiabatic particle behavior was not observed. The reader may recall that according to empirical theory, nonadiabatic particle behavior, if it were to occur, would make itself manifest on plots like figure 16 in a shift of data to the right with increasing ϵ . This point was illustrated in figure 15.

As pointed out earlier, the magnetic field affected the total current emitted as the electron gun was rotated with respect to the magnetic field. However, the angular distribution of the beam remained relatively constant over a range of beam accelerating voltages and magnetic field strengths, as evidenced by the close agreement between the

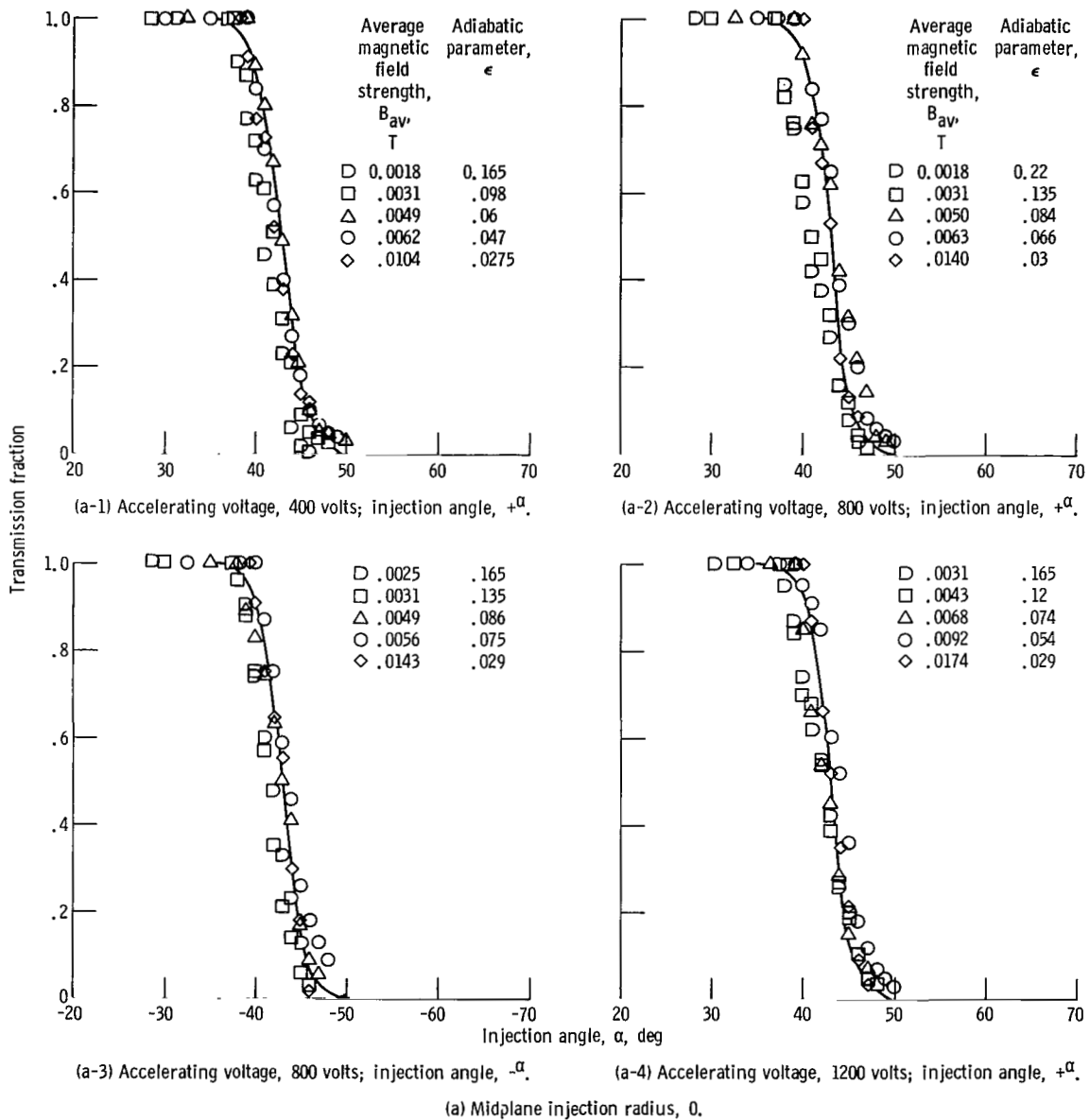
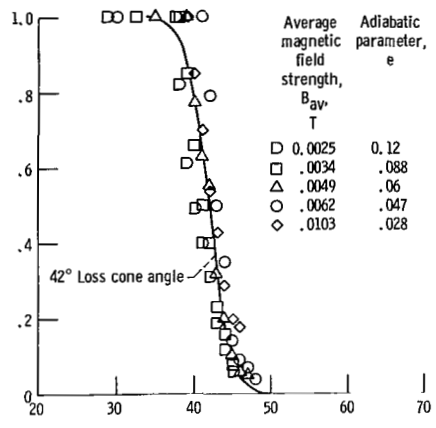
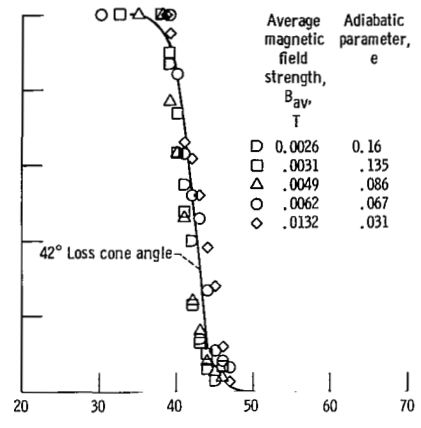


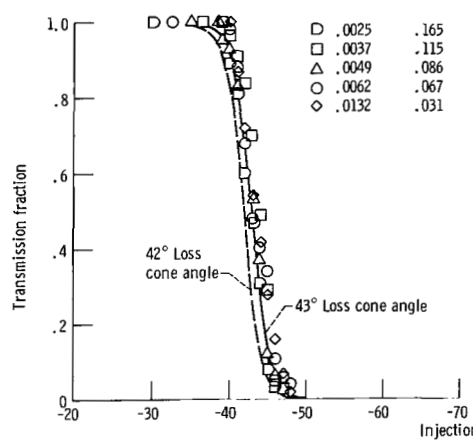
Figure 16. - Electron transmission fraction as function of injection angle α for various average magnetic field strengths and accelerating voltages. Mirror ratio on magnet axis, 0.465. Curve shown is transmission fraction calculated from beam divergence measurements for a loss cone angle of 43° .



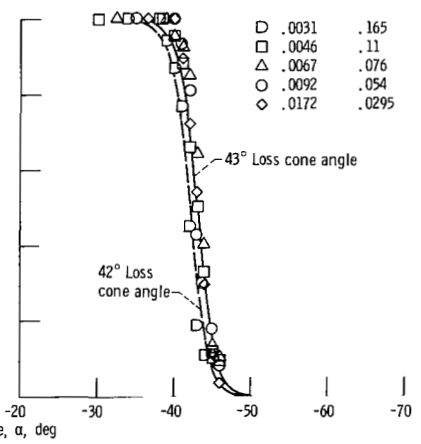
(b-1) Accelerating voltage, 400 volts; injection angle, $+\alpha$.



(b-2) Accelerating voltage, 800 volts; injection angle, $+\alpha$.

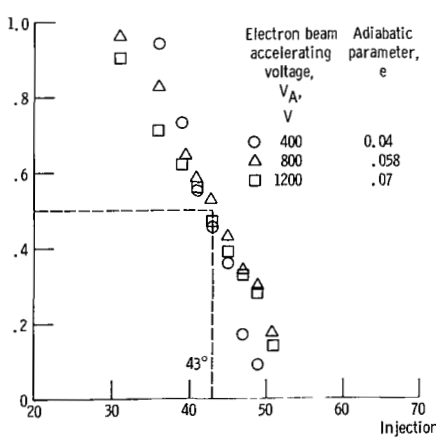


(b-3) Accelerating voltage, 800 volts; injection angle, $-\alpha$.

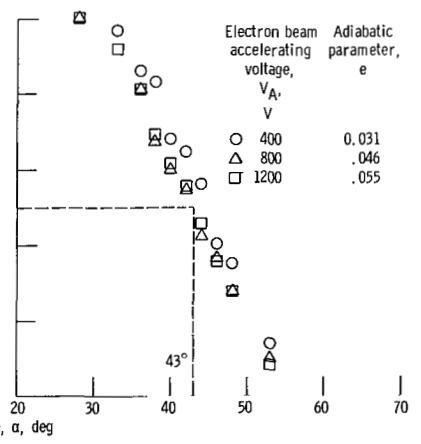


(b-4) Accelerating voltage, 1200 volts; injection angle, $-\alpha$.

(b) Midplane injection radius, 4 centimeters. Curve shown is transmission fraction calculated from beam divergence measurements for loss cone angles of 42° and 43°.



(c-1) Average magnetic field strength, 7.2×10^{-3} tesla.



(c-2) Average magnetic field strength, 9.1×10^{-3} tesla.

(c) For an oxide cathode electron gun; injection radius, 0 at an axial position slightly behind the midplane ($z = -0.5$ cm).

Figure 16. - Concluded.

experimental data and the predicted results.

In figure 16(b), transmission results are presented for electrons injected at the midplane at a radial distance of 4.0 centimeters from the axis and for a range of conditions. The mirror ratio R_m (taking into account the curvature of the magnetic field lines) at a radial distance of 4.0 centimeters is 0.446. The loss cone angle associated with this mirror ratio is 42° (eqs. (6)).

In figure 16(b-1) and (b-2) the transmission results are shown for positive injection angles. The curve calculated from the beam divergence and a loss cone angle of 42° is also plotted on the figures for comparison. Because electrons injected off-axis at positive injection angles gyrate above the injection point, the mirror ratio for this region slightly less than 0.446 resulting in a loss cone angle slightly less than 42° . The experimental results again agree closely with those predicted from beam divergence measurements.

In figure 16(b-3) and (b-4) the data are presented for negative injection angles, where the electrons gyrate below the injection point. In this region the mirror ratio approaches the axial mirror ratio of 0.465 which corresponds to a loss cone angle of 43° . Calculated results are plotted for loss cone angles of 42° and 43° . From theoretical considerations, the data points would be expected to fall between these transmission curves. The actual data points, however, are distributed about the transmission curve for 43° . This slight shift may be data scatter or may be the result of nonadiabatic behavior. For the range of ϵ (0.029 to 0.162) covered by the data of figure 16(b), the loss cone angle did not increase (within the 2° spread of the data).

The transmission results presented in figure 16(c) were obtained with an electron gun positioned on axis ($R = 0$) but slightly behind the midplane ($z = -0.5$ cm). These results were used to identify any change in the transmission characteristics between a particle crossing the midplane and a particle injected at the midplane. A change in the transmission characteristics might be expected because the largest change in the magnitude of the magnetic moment occurs at the midplane. The electron gun used for these measurements was a triode gun with an oxide coated cathode. An anode aperture of 0.15 centimeter resulted in a beam divergence angle as large as $\pm 15^\circ$.

For the tests plotted in figure 16(c-1) and (c-2) the magnetic field was held constant while the beam accelerating voltage was varied. The beam angular distribution increased with accelerating voltage as evidenced by the changing slope of the transmission measurements. The slope of the data is constant for each accelerating voltage though, and passes through the 50 percent transmission point at a loss cone angle of 43° . The range of ϵ for figure 16(c-1) extended from 0.04 to 0.07, and for figure 16(c-2) from 0.031 to 0.055. Within this limited range of ϵ , the results indicate that the loss cone angle did not increase as a result of injection slightly behind the midplane.

In summary, the experimental range of ϵ investigated in the course of this effort

was from 0.027 to 0.22. Results of the transmission measurements (fig. 16) indicate that the loss cone did not increase (within the 2° spread of the experimental data). For single interaction with the magnetic mirror region, particle behavior was adequately predicted by adiabatic theory. Values of ϵ considerably larger than 0.22 were not investigated with the experimental apparatus described herein because the required low magnetic field strengths (resulting in large electron gyroradius) would lead to electrons striking the magnet coil. This was found by test to occur at an $\epsilon = 0.35$. Values of ϵ below 0.02 required magnetic field strengths that distorted the distribution of the electron beam.

Previous results (ref. 13) for single interaction with a magnetic mirror using much larger magnetic fields indicated that a transition to nonadiabatic behavior would be expected for $\epsilon = 0.046$ at $R = 0$ and for $\epsilon = 0.041$ at $R = 4.0$ centimeters for a mirror ratio of 0.465. In the range of values tested and reported herein, which extends both above and below the indicated adiabatic transition value of ϵ , no evidence of an increase in the loss cone was found.

CONCLUDING REMARKS

Nonrelativistic single particle behavior was experimentally investigated in an axisymmetric mirror magnetic field. Measurements were made on an electron beam for a single interaction with the mirror region. Within the 2° spread of data of this investigation, the loss cone angle for a single interaction of electrons with a mirror field was not observed to increase (i. e., to become noticeably nonadiabatic) for a range of the adiabatic parameter ϵ from 0.027 to 0.22.

Lewis Research Center,
National Aeronautics and Space Administration,
Cleveland, Ohio, June 25, 1970,
120-26.

APPENDIX - SYMBOLS

a	nondimensional radius, $\pi R/z_0$	r_g	particle gyroradius, mv_{\perp}/qB_0
B_{av}	average magnetic field strength (eq. (5)), T	T	fraction of electron beam transmitted through mir- ror region, I_O/I_I
B_{max}	maximum axial magnetic field strength, T	V_A	electron beam accelerating voltage, V
B_{min}	minimum axial magnetic field strength, T	v_{\parallel}	particle velocity parallel to magnetic field, m/sec
B_0	axial magnetic field strength, T	v_{\perp}	particle velocity perpendic- ular to magnetic field, m/sec
C_1, C_2, C_3	constants defined in eqs. (1) to (3)	z	axial distance from mid- plane, cm
I_I	electron current measured inside magnetic mirror region, A	z_0	axial distance between B_{min} and B_{max} , cm
I_O	electron current measured outside magnetic mirror region, A	α	particle injection angle, deg
J_0, J_1, J_2	longitudinal adiabatic in- variant terms (eq. (2))	δ	beam divergence half-angle, deg
M_0, M_1, M_2	magnetic moment adiabatic invariant terms (eq. (1))	ϵ	adiabatic parameter (eq. (4)), $mv_{\perp}/qB_{av}z_0$
m	electron mass, kg	θ_0	loss cone half-angle, deg
q	electronic charge, C	Φ_0, Φ_1, Φ_2	flux adiabatic invariant terms (eq. (3))
R	particle injection radius, cm		
R_m	mirror ratio on magnet axis, B_{min}/B_{max}		

REFERENCES

1. Artsimovich, L. A. (P. Kelly and A. Peiperl, trans.): *Controlled Thermonuclear Reactions*. Gordon and Breach Science Publ., 1964.
2. Northrop, Theodore G.: *The Adiabatic Motion of Charged Particles*. Interscience Publ., 1963.
3. Glasstone, Samuel; and Lovberg, Ralph H.: *Controlled Thermonuclear Reactions. An Introduction to Theory and Experiment*. D. Van Nostrand Co., Inc., 1960.
4. Milder, Nelson L.; and Kaufman, Harold R.: *Analysis of Electron Analog Simulation of Ion Containment in Magnetic Fields*. NASA TN D-5217, 1969.
5. White, Elmer: *Analytical and Experimental Charged-Particle Trajectories in Mirror-Cusp Magnetic Fields*. Rep. AFAPL-TR-67-91, Air Force Aeropropulsion Lab., Feb. 1968. (Available from DDC as AD-669055.)
6. Siambis, J. G.; and Trivelpiece, A. W.: *Adiabatic Containment of Charged Particles in Combined Mirror-Multiple Cusp Magnetic Fields*. *Phys. Fluids*, vol. 8, no. 11, Nov. 1965, pp. 2047-2058.
7. Dragt, A. J.: *Trapped Orbits in a Magnetic Dipole Field*. *Rev. Geophys.*, vol. 3, no. 2, May 1964, pp. 255-298.
8. Alfvén, Hannes; and Faelthammar, Carl-Gunne: *Cosmical Electrodynamics. Fundamental Principles*. Second ed., Clarendon Press, Oxford, 1963.
9. Burns, Joseph A.; and Halpern, Gerald: *Dynamics of a Charged Particle in a Spiral Field*. *J. Geophys. Res.*, vol. 73, no. 23, Dec. 1, 1968, pp. 7377-7384.
10. Garren, A.; Riddell, R. J.; Smith, L.; Bing, G.; Henrich, L. R.; Northrop, T. G.; and Roberts, J. E.: *Individual Particle Motion and the Effects of Scattering in an Axially Symmetric Magnetic Field*. *Theoretical and Experimental Aspects of Controlled Nuclear Fusion*. Vol. 31 of the Proceedings of the Second United Nations, International Conference on the Peaceful uses of Atomic Energy. United Nations, 1958, pp. 65-71.
11. Rodionov, S. N.: *An Experimental Test of the Behaviour of Charged Particles in an Adiabatic Trap*. *J. Nucl. Energy, Pt. C: Plasma Phys.*, vol. 1, no. 4, July 1960, pp. 247-252.
12. Gibson, G.; Jordan, W. C.; and Lauer, E. J.: *Particle Behavior in Static, Axially Symmetric, Magnetic Mirror and Cusp Geometries*. *Phys. Fluids*, vol. 6, no. 1, Jan. 1963, pp. 116-133.

13. Roth, J. Reece: Nonadiabatic Particle Losses in Axisymmetric and Multipolar Magnetic Fields. NASA TN D-3164, 1965.
14. Balebanov, V. M.; and Semashko, N. N.: Lifetime of Individual Charged Particles in a Magnetic Mirror Trap. Nucl. Fusion, vol. 7, Dec. 1967, pp. 207-218.
15. Dubinina, A. N.; Krasitskaya, L. S.; and Yudin, Yu. N.: Motion of Charged Particles in a Magnetic Trap with a Mirror Configuration. Plasma Phys., vol. 11, no. 7, July 1969, pp. 551-564.
16. Fukui, Shuji; Hayakawa, S.; Honzawa, T.; Nishimura, H.; and Obayashi, H.: Loss Mechanism of Electrons from a Magnetic Bottle. J. Phys. Soc. Japan, vol. 20, no. 8, Aug. 1965, pp. 1487-1496.
17. Dubinina, A. N.; Trainin, L. Ya; and Chirikov, B. V.: Trap with Magnetic Mirrors, Designed for Prolonged Electron Confinement. Soviet Phys. -JETP, vol. 22, no. 2, Feb. 1966, pp. 260-263.
18. Eubank, H. P.: Single-Particle Confinement Studies in a Radio-Frequency-Supplemented Magnetic Mirror. Phys. Fluids, vol. 12, no. 1, Jan. 1969, pp. 234-240.
19. Keller, Thomas A.; and Wise, George A.: Experimental Results of a 1500-Cubic-Foot Unbaked Ultrahigh Vacuum System. High-Vacuum Technology, Testing, and Measurement Meeting. NASA TM X-1268, 1966, pp. 19-25.
20. Schertler, Ronald J.: Outgassing Characteristics of an Epoxy-Impregnated Magnet Coil. NASA TM X-1813, 1969.
21. Brown, Gerald V.; and Flax, Lawrence: Superposition Calculation of Thick Solenoid Fields From Semi-Infinite Solenoid Tables. NASA TN D-2494, 1964.
22. Crawford, C. K.: Improved Series of Ion Gun Parts. Rev. Sci. Inst., vol. 36, no. 6, June 1965, p. 844.
23. Harker, Kenneth J.: Use of Scanning Slits for Obtaining Current Distribution in Electron Beams. J. Appl. Phys., vol. 28, no. 11, Nov. 1957, pp. 1354-1357.
24. Moss, Hilary: Narrow Angle Electron Guns and Cathode Ray Tubes. Supplement 3 of Advances in Electronics and Electron Physics. Academic Press, 1968.

FIRST CLASS MAIL



POSTAGE AND FEES PAID
NATIONAL AERONAUTICS AND
SPACE ADMINISTRATION

06U 001 49 51 3DS 70272 00903
AIR FORCE WEAPONS LABORATORY /WLOL/
KIRTLAND AFB, NEW MEXICO 87117

ATT E. LOU BOWMAN, CHIEF, TECH. LIBRARY

POSTMASTER: If Undeliverable (Section 158
Postal Manual) Do Not Return

"The aeronautical and space activities of the United States shall be conducted so as to contribute . . . to the expansion of human knowledge of phenomena in the atmosphere and space. The Administration shall provide for the widest practicable and appropriate dissemination of information concerning its activities and the results thereof."

— NATIONAL AERONAUTICS AND SPACE ACT OF 1958

NASA SCIENTIFIC AND TECHNICAL PUBLICATIONS

TECHNICAL REPORTS: Scientific and technical information considered important, complete, and a lasting contribution to existing knowledge.

TECHNICAL NOTES: Information less broad in scope but nevertheless of importance as a contribution to existing knowledge.

TECHNICAL MEMORANDUMS: Information receiving limited distribution because of preliminary data, security classification, or other reasons.

CONTRACTOR REPORTS: Scientific and technical information generated under a NASA contract or grant and considered an important contribution to existing knowledge.

TECHNICAL TRANSLATIONS: Information published in a foreign language considered to merit NASA distribution in English.

SPECIAL PUBLICATIONS: Information derived from or of value to NASA activities. Publications include conference proceedings, monographs, data compilations, handbooks, sourcebooks, and special bibliographies.

TECHNOLOGY UTILIZATION PUBLICATIONS: Information on technology used by NASA that may be of particular interest in commercial and other non-aerospace applications. Publications include Tech Briefs, Technology Utilization Reports and Notes, and Technology Surveys.

Details on the availability of these publications may be obtained from:

SCIENTIFIC AND TECHNICAL INFORMATION DIVISION
NATIONAL AERONAUTICS AND SPACE ADMINISTRATION
Washington, D.C. 20546